Towards a new transfer standard for speed of sound measurements in liquids at cryogenic temperatures

A new transfer standard for speed of sound measurements in liquids at cryogenic temperatures.

G. Cavuoto[a], S. Lago[a], P. A. Giuliano Albo[a]

[a]*Istituto Nazionale di Ricerca Metrologica (INRiM), Strada delle Cacce 91, 10135 Torino, Italy*

Abstract

Measurement of fluids flows represents an unparalleled tools for the account of the transferred mass, heat and energy; however, considering the wide ranges of transported fluids flow-rates, temperatures, pressures, viscosity and densities, high accurate calibrations of ultrasonic flowmeters remain demanded. As an alternative to the usual gravimetric calibration, there is a less explored possibility to provide the traceability of the measurement through the speed of sound.

In this work an ultrasonic sensor, which operates on the basis of the *double pulse-echo* technique is presented. This sensor is capable to provide measurements of speed of sound, fully traceable to units of length and time. Moreover, it has been optimized to operate when set both into a laboratory thermostat and into industrial plants using spools like DN50, or larger, in order to be adopted as a transfer standard for flow rate measurements. The concept behind this idea is the possibility of characterising the ultrasonic cell, namely the velocity meter, in a controlled temperature and pressure conditions in a laboratory environment. Thereafter, it is possible to connect the sensor directly to the natural gas distribution lines, nearby the industrial ultrasonic flow meters, normally used to monitor the LNG flow. This procedure would bring the significant benefit of enabling industrial flowmeters to be calibrated without the need for prior knowledge of the composition of the fluid under test, as well as avoiding the shutdown or removal of flowmeters during their calibration.

The sensor has been tested and characterized performing measurements in liquid methane in the temperature range of (100 and 162) K and for pressure up to 10 MPa. The expanded relative uncertainty of the obtained speed of sound, w is $U_r(w) = 0.15$ % ($k = 2$) for temperature below 130 K and $U_r(w) = 0.32$ % ($k = 2$) for temperature above 130 K. The obtained values are in agreement with those available in the scientific literature and with the predictions of the Seitzmann and Wagner and GERG equation of state. Along with experimental speed of sound measurements, a deep insight of the procedures adopted to improve the stability of the sensor, the specific corrections applied considering the cryogenic working conditions and a complete analysis of the uncertainty affecting the obtained results is also discussed.

Keywords: Speed of sound, transfer standard for ultrasonic flowmeters, liquid methane.

1. Introduction

Due to practical and cost limitations of the calibration facilities, it is commonly accepted that flowmeter sensors are calibrated in sub-ranges of flow, temperature and pressure, where very controlled con-

Email address: g.cavuoto@inrim.it (G. Cavuoto)

ditions are possible. Then, they can operate in a wider states by applying corrections, as reported in ISO 12242 standard [1]. The side effect of this disjunction is the possible manifestation of incoherent and misinterpreted *on-site* measurements that are amplified when the economic value of transferred fluid is higher.

In the market of liquefied natural gas (LNG), flowmeters calibration conditions are of particular difficulty, due to the absence of facilities operating with pure methane, or LNG, at cryogenic conditions. At the moment, there are only few facilities able to operate at cryogenic temperatures and, mainly, using liquid nitrogen [2-3]. Probably soon, there will be the possibility to operate with LNG and the situation will improve but, even in this case, the calibration procedure will request to stop the line at the production site, to dismount and to deliver flowmeters, periodically. The complete stop of the industrial plant is usually prevented by creating a second measurement line that can operate when the first is under maintaining. This approach solves the problem of continuity, but does not eliminate eventual effects caused by influencing quantities (i.e composition, temperature, pressure, heat flows, etc.), that can be different at working site and at the calibration facility.

Desiderably, in a near future, calibrations shall be performed *on-site* adopting transfer standards, when possible. This approach will allow to reduce costs, to eliminate the effects of influence quantities and it will give the possibility to verify sensors more often, in order to guarantee better performances of gauges over the time.

Among available flowmeters types, ultrasonic sensors are those promising the quickest evolution in terms of *on-site* calibration. Using these meters, composing the upstream and dowstream times of flight of ultrasonic bursts, it is possibile to determine the speed of the flowing mass and the speed of sound of the fluid, as it was at rest. The latter can be used to check the status of the fluid when compared with reference values. Foe example, in the case of binary mixtures, when accurate predictions are available, it is possible to determine the fluid composition. Conversely, it is possible to verify the stability of the sensor in terms of calibration, when reference values are compared with those provided by gauges.

The ISO 12242 standard specifies requirements and recommendations for ultrasonic liquid flowmeters and states that sensors can perform self-tests without the need of repeated and costly full calibrations services. The possibility to calibrate ultrasonic flowmeter using reference values of speed of sound is only slightly tackled in the ISO standard, probably in reason of a limited possibility of application of such approach. As a matter of fact, reference speed of sound measurements are available only for a very limited number of fluids, many of them at purity grades not found on industrial plants.

This work would represent a preliminary contribution for investigating the possibility to realize a transfer standard for speed of sound. Today speed of sound measurements can be made traceable to unit of length and time [4] and, thanks to hundreds of scientific papers, sensors performances have been proved to be mainly independent from measured fluids. As a first step, the complete traceability of a speed of sound measurement cell must be proved even when the sensor is calibrated at ambient conditions but measurements are performed at very different temperatures and pressures. This approach would allow to focus development efforts on the technological improvements of the transfer standard instead of many different classes of ultrasonic flowmeters. A calibrated speed of sound cell

could be installed on permanent ultrasonic flowmeters to provide needed reference values, at the same temperature, pressure and composition, whatever the flowing fluid is. The same transfer standard could be adopted for the calibration of temporary ultrasonic flowmeters (i.e. clamp-on) in laboratory, where, thanks to provided reference values, it would be possible to determine almost all the parameters needed to calibrate the sensor without making use of independent propagation models of the sound in the wedges.

Methane provides advantages with respect to other possible alternative choices because, being a pure substance, it can be easily reproduced at a know level of purity; it is the main component of LNG and thus both the speed of sound, the acoustic impedance and the signal wavelength are only slightly different from those of LNG. Furthermore, scientific literature is plentiful of papers investigating thermodynamic properties of methane and, in particular, there are several works dedicated to speed of sound measurements [6-10].

Despite this, surprisingly, there are few studies focused on determining the speed of sound of methane at cryogenic temperatures. Specifically, since the second half of the 1960s until the end of the 1980s, only four works reported experimental results within the pressure range involved in the custody transfer process of LNG. These contributions [11–14] are listed in Table 1, where adopted experimental techniques, temperatures and pressures ranges and the declared uncertainties are shown.

Authors	Technique	T / K	p / MPa	Declared uncertainty / %
Van Itterbeek, Thoen (1967)	Pulse superposition technique	111- 190	0.1-18	0.1
Singer (1969)	double pulse-echo	94 - 145	0.2 - 9	0.5
Straty (1974)	Pulsed technique	91 - 300	1.6 - 35	(0.05 - 0.2)
Baidakov (1982)	Pulsed technique	150 - 183	<4	(0.1 - 0.3)

Table 1: List of experimental works on speed of sound measurements of methane at cryogenic temperature.

Demand of investigation of new *on-line* calibration approaches are particularly persistent in the field of LNG flowmetering in reason of the economic value of the transferred fluid and the limited possibility to calibrate flowmeters at real operating conditions. For this reason, in a first attempt, a speed of sound measurement cell has been built and tested in the temperature range of (130 and 160) K when immersed in liquid methane at pressure up to 10 MPa [5]. That preliminary work showed that the performances of the cell were comparable with the best results available in literature, but they were still not sufficient to consider the sensor suitable as a transfer standard, in particular, at temperatures below 140 K, where the main problem was the limited repeatability of the measurements after tens temperature cycles from cryogenic to ambient conditions. To improve the mechanical stability of the sensor, some components have been modified and the repeatability has been improved to better than 0.05 %, therefore in the order of magnitude expected for a cell working at ambient temperature. Thanks to these modifications

of the ultrasonic cell, the stability of the measurement and its repeatability have also been improved, reducing the uncertainty associated with the speed of sound from 0.42 % of the previous work, to 0.15 % of the new measurements. Encouraging progresses inspired this work where the sensor performances are investigated extending the temperature range form 100 K to 160 K, in this way, the thermodynamic conditions found on industrial plants have been completely covered.

2. Measurement technique and corrections

Among possible measurement methods, it has been chosen to approach the realization the transfer standard by implementing the *double pulse-echo*, since it is a well established, documented and already successfully adopted in different research contexts. In this frame, the measurement of the speed of sound is obtained by measuring the delay time between two signals, emitted simultaneously, traveling different path lengths at the same speed. Exhaustive descriptions of the measurement principle and its implementation can be found in [4, 17-19] where also main corrections to the measurements are described.

For a correct designing of the sensor that have to perform at cryogenic conditions, it is useful to take some few precaution. For example, it is necessary to have an accurate model for the thermal expansion coefficient of the measurement cell and to avoid geometries for which the thermal stress can generate plastic deformations or failures of the sensor parts. Ultrasonic signals are generated by a piezoelectric disk that is maintained in its position by a clamping system. Being particularly robust, and able to absorb the mechanical and thermal stresses, it has been chosen to adopt a polymer-encapsulated piezoelectric source, so the piezoelectric doesn't break if thermally stressed. Failures of the ultrasonic generation system have never been observed and calibration parameters of the sensor compared favorably even after many tens of temperature cycles from ambient to cryogenic conditions.

After having evaluate different materials (ranging from grade 5 titanium to stain-less invar) to build the measurement cell, the choice fell on AISI-316L stain-less steel, because it is chemical stable and for its acoustic and mechanical properties.

Preserving the cylindrical symmetry of the cell spacers, reflectors and the source support, corrections for temperature and pressure can be calculated with the necessary accuracy even for variations of hundreds kelvin and megapascal.

Speed of sound is calculated measuring the difference of the paths length $\Delta L = L_2 - L_1$ and the delay time τ as:

$$w_{\text{exp}} = \frac{2\Delta L}{\tau + \delta\tau} \tag{1}$$

where $\delta\tau$ is the correction to the delay time due to diffraction of the ultrasonic signals [17].

2.1. Temperature and pressure corrections

To compensate the effect of deformation occurring when temperatures and pressures are very different from those measured during calibration, the following differential equations have been used:

$$\left(\frac{\partial \Delta L(T,p)}{\partial T}\right)_p = \alpha(T)\Delta L(T,p) \tag{2}$$

$$\left(\frac{\partial \Delta L(T,p)}{\partial p}\right)_T = \frac{\beta_T}{3}\Delta L(T,p) \tag{3}$$

where β_T and α are the isotermal compressibility and the thermal expansion coefficient of the AISI-316L stainless steel respectively.

Performing measurements at cryogenic conditions, it is worth to consider, at least, the dependency of α from temperature and, hereafter, it is reported the expression suggested by NIST [20] for AISI-316L:

$$\alpha(T) = a + bT + cT^2 + dT^3, \tag{4}$$

where coefficients are $a = 5.867532{\cdot}10^{-7}$, $b = 1.405386{\cdot}10^{-7}$, $c = 5.263604{\cdot}10^{-10}$, $d = 7.604209{\cdot}10^{-7}$.
Solving the differential equations in terms of ΔL the following expression is obtained:

$$\Delta L(T,p) = \Delta L(T_0,p_0)\left(1 + \alpha(T)\exp(\gamma) - \frac{\beta}{3}(p-p_0)\right), \tag{5}$$

where $\Delta L(T_0,p_0)$ is the difference of paths length measured at ambient temperature, and atmospheric pressure, while $\gamma = (a(T-T_0) + \frac{b}{2}(T^2-T_0^2) + \frac{c}{3}(T^3-T_0^3) + \frac{d}{4}(T^4-T_0^4)$.

2.2. Temperature gradient corrections

Though, in laboratory conditions, temperature gradients can be controlled by heat compensators, the same could not happen during *on-site* calibrations. In the case, the experimental time of flight τ_{exp} can be corrected to minimize the effect of any residual temperature gradient which takes place along the measurement cell. The corrected delay time can be calculated, using the experimental delay time τ_{exp} and speed of sound w_{exp}, using the following expression:

$$\tau_g = \tau_{exp}\left(1 + \frac{a}{\tau_{exp} w_{exp}^2}(L_2^2 - L_1^2)\right), \tag{6}$$

where

$$a = \frac{\partial w}{\partial z} = \frac{\partial w}{\partial T}\frac{\partial T}{\partial z} \tag{7}$$

is the sensitivity coefficient of the correction accounting for the variation of the speed of sound due to the temperature and the temperature gradient. In the same expression, the coordinate z is identified by the logitidinal axis of the measurement cell.

2.3. Diffraction corrections

The wavy nature of the ultrasonic signals imposes further corrections to the delay time because received signals are not necessary in phase with each other due to the limited dimension of the source. Though, only an infinitely small or infinitely large source would generate perfectly phased signals, it is possible to design the measurement cell combining source diameter and acoustic paths length in a way that diffraction corrections remains small compared to other source of uncertainty [17].

The corrections $\delta\tau$ can be calculated using the following expressions as reported in [17] and elaborated in [21]:

$$\delta\tau = \frac{\phi(2L_2) - \phi(2L_1)}{\omega_0}, \tag{8}$$

$$\phi(L) = \mathrm{Arg}\left[1 - \exp\left(-\frac{i2\omega b^2/w_{\mathrm{exp}}}{2L}\right)\left(\mathrm{J}_0\left(\frac{2\omega b^2/w_{\mathrm{exp}}}{2L}\right) + i\mathrm{J}_1\left(\frac{2\omega b^2/w_{\mathrm{exp}}}{2L}\right)\right)\right]. \tag{9}$$

where b is the radius of the source, J_0 and J_1 are Bessel functions of zero and first order, respectively, and $\omega = 2\pi/f$ with f the carrier frequency of the signal.
Combining the corrections of the delay time, the actual time of flight is calculated as:

$$\widetilde{\tau} = \tau_{\mathrm{g}} + \delta\tau \tag{10}$$

while the corrected speed of sound $\widetilde{w}$ is evaluated taking into account the corrected acoustic path length, by expression (5), and the corrected time of flight, by expression (6), as reported in the following equation.

$$\widetilde{w} = \frac{2\Delta L(T,p)}{\widetilde{\tau}}. \tag{11}$$

3. Experimental apparatus for cryogenic speed of sound measurements

The core element of the apparatus is a 75 mm long ultrasonic cell made of stainless steel AISI 316L, which includes two spacers of different lengths. As pictured in Figure 1, the piezoelectric source is clamped by the support using four screws, gray in the picture, that have been shortened. The measuring cell is hosted in the control system of the temperature and of the pressure. As shown in figure 2 number 11, the sensor is hanged on the upper flange of the AISI-316L pressure vessel, that is able to operate up to 70 MPa.

To properly perform in the range of 100 K and 160 K, the temperature control system has been designed to compensate for unwanted heat flows from the ambient in the form of radiation (typically small but measurable) and thermal conductivity (the main contribution). To the scope, liquid nitrogen has been flowed into a cylindrical heat exchanger (11 in figure 2), made of aluminum, that is cooled down to approximately 80 K. The inner surface of the heat exchanger is in thermal contact with a copper shield (7 in figure 2), equipped with an electrical heater, used to regulate the heat flow coming from the

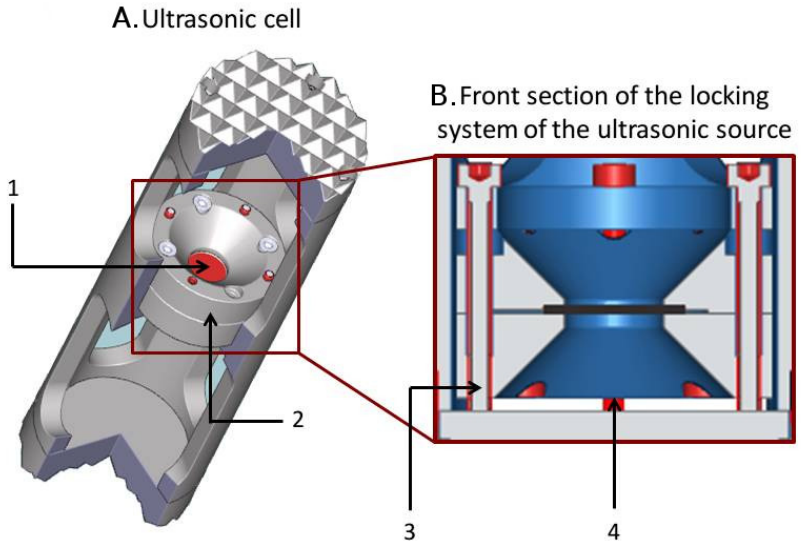

Figure 1: Ultrasonic cell and front section of the piezoelectric disk locking system. (1) Piezoelectric disk. (2) Stainless steel locking system. (3) Steel screw to secure the locking system to the ultrasonic cell. (4) Screws exceeding part.

pressure vessel (3 in figure 2), that is set inside. An aluminum thermal bridge has been set on the top of pressure vessel and it has been used to precondition the temperature of the gas and to reduce the heat flows coming from the ambient through the high pressure circuit. Being separately controlled, if necessary, the bridge can be maintained at a different temperature with respect to that of the pressure vessel. Though the describe system is much simpler than those adopted for traditional cryostats, the reached temperature stability was better than ±25 mK and the temperature gradient from the top to the bottom of the pressure vessel never exceeded 80 mK, in the worst case.

Figure 3 shows the scheme of the complete experimental apparatus. The control ring is closed by a personal computer connecting actuators (two power supplies for electric heaters, a power supply for the liquid nitrogen valve and a function generator to excite the ultrasonic source) and monitors (four multimeters measuring the temperatures of the vessel, the of thermal shield, of the bridge and the pressure of the sample). The traceability of the speed of sound measurements is guaranteed by the calibration certificates of the thermometers, the pressure transducer, the time-base of the oscilloscope and of the cell paths lengths.

In particular, temperature of measuring cell is obtained as the mean value of the resistances measured by two PT100 placed inside the walls of the pressure vessel, (9 and 13 in figure 2). These thermometers are calibrated by using the international temperature scale ITS-90 [22], using the triple point of argon, the triple point of mercury and the triple point of water, as calibration points, with an uncertainty of ±0.02 K. The pressure of the liquid methane is measured by a temperature controlled pressure transducer (Honeywell Super TJE) placed on the inlet line of methane and calibrated with an accuracy of ±0.025 MPa,

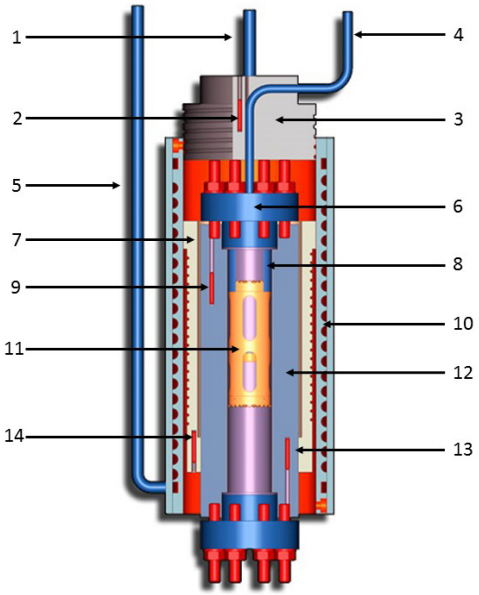

Figure 2: Cryogenic thermal apparatus: (1) LN_2 inlet; (2) Aluminium bridge thermometer, PT100; (3) Aluminium bridge; (4) CH_4 inlet; (5) LN_2 outlet; (6) Vessel stopper; (7) Thermal shield; (8) Coupling holders; (9) Upper thermometer, PT100; (10) Heat exchanger; (11) Measuring cell; (12) Pressure vessel; (13) Lower thermometer, PT100; (14) Thermal shield thermometer, PT100.

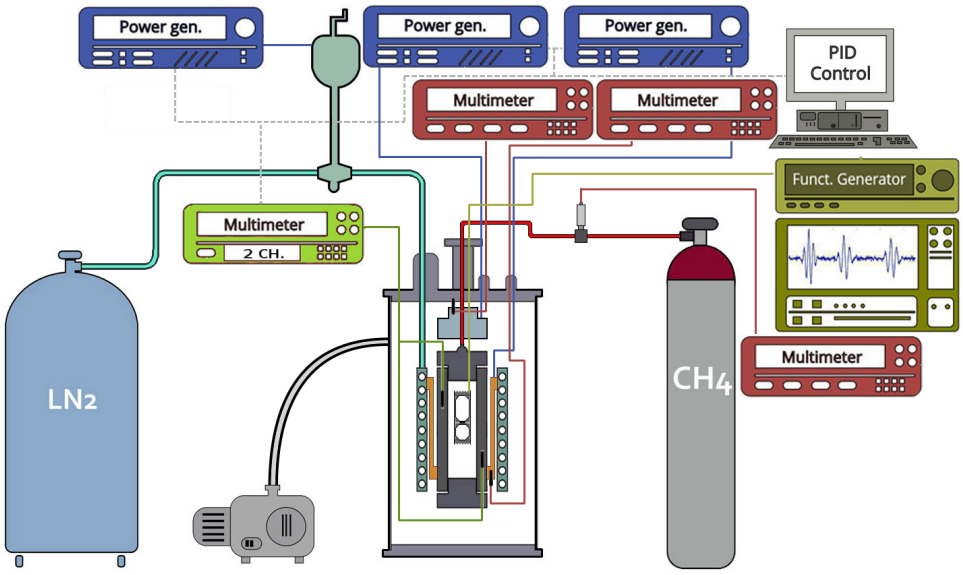

Figure 3: Cryogenic apparatus for speed of sound measurements.

up to 50 MPa. The whole apparatus is thermally isolated from the environment by a vacuum chamber, that is evacuated at a pressure of about $5 \cdot 10^{-3}$ mbar. The experimental apparatus is also deeply described in Cavuoto *et al.* [5] where further details on thermal control and on the measurement procedures are discussed.

4. Ultrasonic cell improvement

Though the speed of sound measurements obtained in this work and those of Cavuoto *et al.* [5] showed good agreement for temperature down to 140 K, at lower temperature, consistency of the measurements was not good as expected. In fact, that first work aimed to test materials and measurements procedures for temperatures between (130 and 162) K and pressures up to 10 MPa and the results showed deviations of up to 1.5 % from the values predicted by the equations of state for temperatures below 140 K. Moreover, at lower temperatures, the experimental values were not consistent with the speed of sound data available in the literature and used as reference values. For this reason, the performances of the cell has been verified alternating cryogenic temperature cycles and cell calibration using water as reference fluid. Usually the repeatability of the calibration is better than 50 parts per million (ppm) of the acoustic path lengths, however, in this case it was 50 times worse and degraded after each temperature cycle. Since, during thermal cycles, the most thermally stressed parts of the sensor are the screws used to fix the ultrasonic source, it has been decided to try to substitute them but without success. After some trials, it has been found that the problem could be solved by reducing the length of those screws.

After some investigations it turned out that, due to a design deficiency, the ultrasonic cell suffered the effects of plastic deformation during the cooling and subsequent heating processes taking place in the measurement cycles. In particular, it has been found that four screws, used to assemble the different parts of the ultrasonic sensor, have been stretched too much by the heating system and have been plastically deformed. This caused a leverage effect between the two spacers of the cell, and the acoustic path of the ultrasonic wave varied from time to time, particularly when the temperature was lower. Furthermore, the piezoelectric disk was mounted inside the measuring cell through a clamping system consisting of two AISI 316L stainless steel supports, screwed together firstly, and then fastened to the cell as shown in Figure 1 (B). A careful check showed that their length was such that, after a few measurement cycles, they have been plastically deformed and extended, backing at room temperature. In that condition, they pushed against the support of the cell used to fix the piezoelectric. The resulting effect was that the relative position of the acoustic source, with respect to the reflective walls of the cell, changed from time to time, becoming more evident and sensible to the temperature excursion and the number of thermal cycles.

Moreover, it has been observed that generally, during the disassembly operations of the cell, all the screws had undergone plastic deformations. As a matter of fact, though the repeatability of the measurements was batter than 500 ppm, also after tens of thermal cycles, when dismounted and remounted, the repeatability of the successive measurements become 5 times worse, when using the same screws.

For this reason, re-calibration of the cell is strictly necessary every time the screws have been removed and substituted while, in other cases, the cell can support tens of thermals cycles without showing degrad-

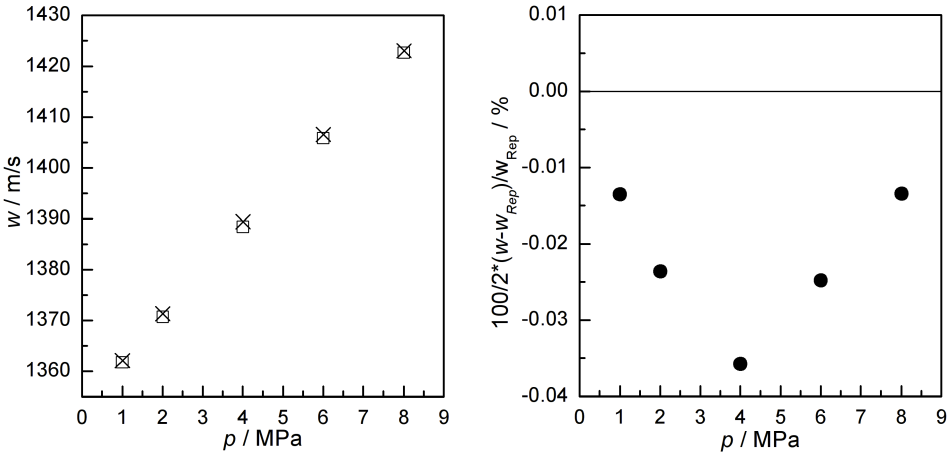

Figure 4: Absolute speed of sounds measured two times at 110 K for pressures up to 8 MPa. (□) First measurement at 110 K; (×) repeated measurement; (•) percentage value of the two measurements repeatability.

ing performances. Purely by way of example, figure 4 shows the results of two repeated measurements at 110 K, when screws have been replaced and the cell have been re-calibrated. The agreement was better that 0.04 % and probably perturbed by different stability conditon of the measurement system. As a matter of fact, when mounting problems had occurred the repeatability would be an order of magnitude worse.

In this work, the cell has been redesigned to have shorter screws, with respect to the ones previously used, and plastic deformations did not occur anymore. The new speed of sound measurements obtained in this new configuration have shown to be more consistent both with the experimental data in the literature and with the predictions provided by the equations of state, proving that the construction defects, detected in the previous experiment, was the source of observed deviations, especially at lower temperatures.

5. Uncertainty analysis

Since the speed of sound $w(T, p)$ is obtained by the independent determinationd of both the acoustic path, ΔL, and the delay time, τ, and through the measurements of the temperatures, T, and the pressures, p, at which the measurements have been carried out, it is possible to estimate its uncertainty by using the following expression for error propagation:

$$\frac{\sigma(w)}{w} = \sqrt{\left(\frac{\sigma(\Delta L)}{\Delta L}\right)^2 + \left(\frac{\sigma(\tau)}{\tau}\right)^2 + \left(\frac{\sigma(T)}{w}\frac{\partial w}{\partial T}\right)^2 + \left(\frac{\sigma(p)}{w}\frac{\partial w}{\partial p}\right)^2 + R^2}, \tag{12}$$

where R is the relative repeatability of the measurements.

The uncertainty associated with time of flight $\sigma(\tau)$ has been obtained as the double of the oscilloscope sampling interval; while the temperature uncertainty is 0.02 K, namely the uncertainty of the platinum

Uncertainty source	Contribution / %
Temperature above 130 K	
Acoustic path length	0.026
Time of flight	0.004
Temperature	0.116
Pressure	0.104
Repeatability	0.036
Estimated expanded uncertainty (k=2)	< 0.32
Temperature below 130 K	
Acoustic path length	0.026
Time of flight	0.004
Temperature	0.056
Pressure	0.0282
Repeatability	0.036
Estimated expanded uncertainty (k=2)	< 0.15

Table 2: List of the uncertainty sources for the calculation of the overall uncertainty (with k = 2) of speed of sound for temperatures above 130 K and below 130 K.

resistance thermometers (PT100) used in this experiment. The pressure uncertainty is 0.025 MPa and, finally, the temperature and pressure dependency terms, $\partial w/\partial T$ and $\partial w/\partial p$, are obtained by fitting the experimental results. Table 2 reports the main contributions, including the scaling effects of sensitivity coefficients, to the uncertainty of the experimental measurements of speed of sound.

When measurements are performed away from the critical point, the sentivity coefficients have been approximated considering the worst condition over a specific interval. Since it has been observed a factor of two between coefficients below and above 130 K, it has been decided to split the uncertainty budget so that between 100 K and 130 K, the range of interest for industrial purposes, the uncertainty is not overestimated too much.

The repeatability R is estimated to be better than 0.036 % though this value has been observed only once and it is usually much better. Anyway, this contribution to the uncertainty budget is much smaller than others and, reducing it by a factor of two, it produces a decrement of the uncertainty of only 0.01 %.

When pressure sensor, thermometers, time-base and acoustic path lengths of the cell are calibrated against standard references, the obtained speed of sound measurements are fully traceable to the definitions of units of length and time. Being this work only a first step toward the realization of a fully traceable transfer standard, it has been preferred to calibrate the acoustic path lengths by using water as reference fluid. Traceability of the here obtained speed of sound results are thus relative to those of pure water but since the uncertainty contribution of the lengths calibrations is much smaller than those of other sources, a direct calibration can reduce the combined uncertainty only slightly.

When path lengths of the speed of sound sensor are calibrated using a reference fluid, the relative uncertainty associated to the acoustic path determination, $\sigma(\Delta L)/\Delta L$, is calculated as:

$$\frac{\sigma(\Delta L)}{\Delta L} = \sqrt{\left(\frac{\sigma(w_w)}{w_w}\right)^2 + \left(\frac{\sigma(\tau)}{\tau}\right)^2 + \left(\frac{\sigma(T_0)}{w_w}\frac{\partial w_w}{\partial T_0}\right)^2 + \left(\frac{\sigma(p_0)}{w_w}\frac{\partial w_w}{\partial p_0}\right)^2}, \tag{13}$$

where the speed of sound in water, w_w, at ambient temperature, T_0, and atmospheric pressure, p_0, are obtained from the IAPWS-95 formulation [22] and used as reference values.

Finally, the expanded relative uncertainty in speed of sound, with a coverage factor $k = 2$, has been estimate to not exceed 0.32 %, for temperatures above 130 K and 0.15 %, for temperatures below 130 K.

6. Results and comments

The specimen of gaseous methane has been provided by SIAD and stored in a 50 litres cylinder. According to the supplier certification, reported in table 3, the gas was pure at the 99.9995 % mol. and no further purification process has been done.

Chemical name	Source	Initial Mole Fraction Purity	Purification Method	Final Mole Fraction Purity	Analysis Method
Methane (CAS name: 74-82-8)	SIAD, ITALY	0.999995	none	-	-

Table 3: Sample table.

The speed of sound has been measured along seven isotherms (100, 110, 120, 130, 140, 150, 162) K and for pressures up to 10 MPa. For a sake of safety, the pressure vessel has been evacuated and cooled down to a temperature of approximately 15 K below the measurement set point. The operation of under cooling the system allows to reduce the time needed, to the injected gaseous methane, to reach a thermodynamic equilibrium close to the measurement temperature. During the liquefaction process, the pressure was maintained approximately at 10.5 MPa, thus few tenths of megapascal above the starting measurement pressure. The liquefaction processes have been monitored by the signals received from the measurement cell. During the fluid loading, the speed of sound was not measurable till the pressure has reached approximately 6 MPa, when the methane was in gas phase. Once the temperature transitory was exhausted, ultrasonic signals were visible on the oscilloscope though they moved too fast to be analyzed. At the and of the filling process, signals were stable and their time-shifting was correlated with temperature and pressure changes.

After final adjustments of the temperature and pressure, it was possible to start measuring the speed of sound beginning from the highest pressure and reducing it step by step. Vessel depressurization induced an extra-cooling that was compensated automatically by electrical heaters. The thermodynamic equilibrium is reached after one hour, approximately, and the speed of sound measurement lasted between 30 and 40 minutes for each measurement point.

Collected experimental speeds of sound, as reported in table 4 and plotted in figure 5, have been compared with the results available in literature, specifically, with the results of the works listed in table 1. *For a sake of completeness, literature results are reported in table 5 with the corresponding uncertainty values.* The relative deviations are reported in plots 6, for temperature below 130 K, and in plot 7, for

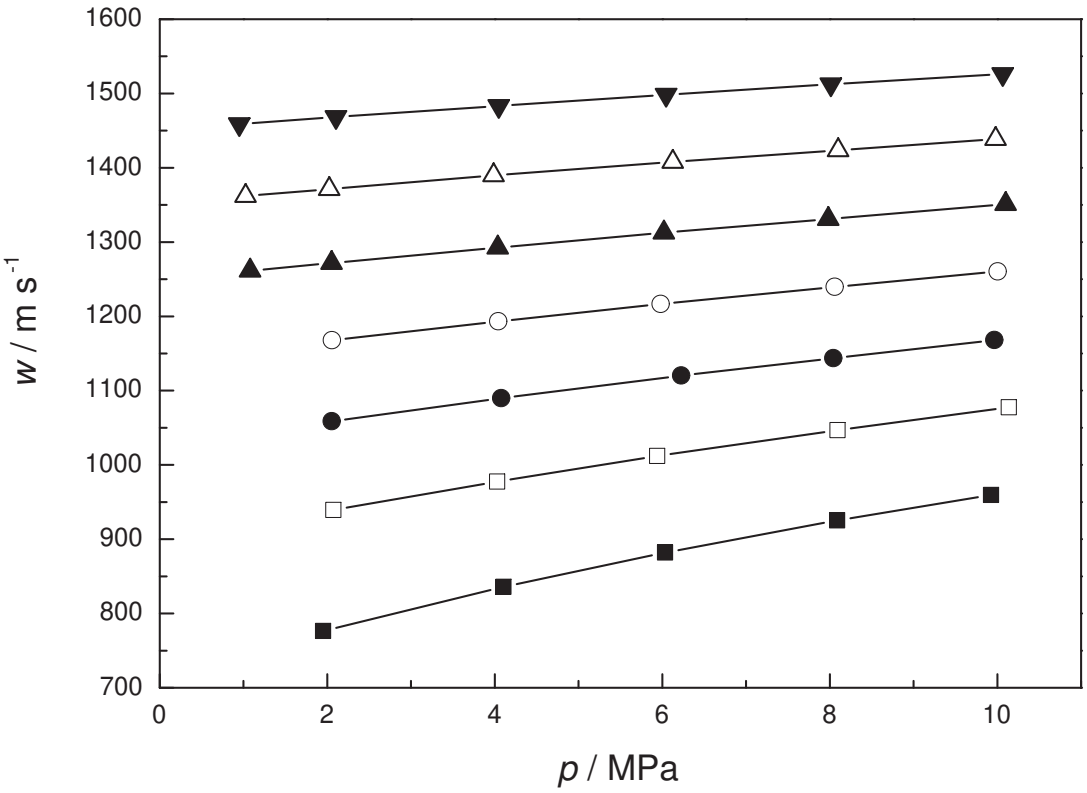

Figure 5: Absolute experimental speeds of sound in liquid methane measured in this work. (▼) T = 100 K; (△) T = 110 K; (▲) T = 120 K; (○) T = 130 K; (●) T = 140 K; (□) T = 150 K; (■) T = 162 K.

T / K	p / MPa	w / m s^{-1}	T / K ($u(T)$ = 0.02 K)	p / MPa ($u(p)$ = 0.025 MPa)	w / m s^{-1} ($U_r(w)$ = 0.32 %)
100.10	0.950	1458.9	140.01	2.055	1058.6
100.09	2.104	1468.3	140.01	4.079	1089.8
100.08	4.047	1483.4	140.03	6.228	1120.2
100.09	6.046	1498.3	140.10	8.044	1143.5
100.11	8.013	1512.4	140.06	9.967	1168.0
100.18	10.064	1526.2			
110.03	1.026	1362.0	150.13	2.073	939.4
110.02	2.024	1371.4	150.15	4.028	977.6
109.95	3.987	1389.8	150.09	5.939	1012.0
109.99	6.124	1407.8	150.08	8.093	1046.9
110.06	8.100	1423.4	150.10	10.137	1077.5
110.02	9.981	1438.7			
120.01	1.079	1261.4	161.85	1.951	776.3
120.02	2.052	1271.7	162.01	4.104	835.9
120.02	4.036	1292.6	162.00	6.035	882.0
120.00	6.019	1312.5	161.97	8.089	925.1
120.07	7.983	1331.0	161.98	9.925	959.4
120.02	10.099	1351.2			
130.03	2.058	1167.7			
130.01	4.043	1193.3			
129.94	5.983	1216.7			
129.99	8.059	1239.8			
130.03	10.007	1260.3			

Table 4: Experimental values of speed of sound in liquid methane. The uncertainty associated to temperature measurements is $u(T)$=0.02 K; that of pressure is $u(p)$=0.025 MPa and the expanded relative uncertainty for speed of sound is $U_r(w)$ = 0.15 % (k = 2) for temperatures below 140 K and $U_r(w)$ = 0.32 % (k = 2) for higher temperatures.

temperature above 130 K.

Lower temperatures comparison shows that, with few exception, the literature results are compatible even if the uncertainty of here obtained values was not considered. In very few other cases, measurements are in agreement within the combined uncertainties and only one of the measurement of Straty at 120 K, and two of Singer at 110 K, are not compatible.

Particular attention should be placed on the agreement between the new measures and the results obtained by Van Itterbeek *et al.* In fact, in Cavuoto *et al.* [5], there was a lack of consistency between the speeds of sound measured at lower temperatures (T < 130 K) and the expected values, that new measurements have recovered.

Similarly, the comparison for temperatures above 130 K shows that the new experimental speeds of sound are all in agreement, within the combined uncertainties, with the results found in literature. The

Author	T / K	p / MPa	w / m s^{-1}	$u_r(w) \cdot 10^2$	Author	T / K	p / MPa	w / m s^{-1}	$u_r(w) \cdot 10^2$
Van Itterbeek *et al.*	125.1	1.0102	1209	0.1	Singer	145.6	8.5808	1100	0.5
	125.1	1.991	1220.8	0.1		145.6	1.824	980	0.5
	125.1	3.9172	1242.7	0.1		124.9	5.884	1260	0.5
	125.1	5.9235	1265.1	0.1		125.1	1.0199	1210	0.5
	125.1	8.7747	1295	0.1		125	7.9434	1282	0.5
	125.1	9.788	1305.2	0.1		125	3.5402	1240	0.5
	111.33	0.9808	1349.6	0.1		125.1	8.7377	1295	0.5
	111.33	1.9728	1358.7	0.1		112	8.7279	1430	0.5
	111.33	3.9324	1376.6	0.1		112.1	6.1292	1400	0.5
	111.33	5.8839	1393.1	0.1	Straty	120	9.258	1345.2	0.2
	111.33	7.569	1408.5	0.1		120	4.367	1290.5	0.2
	140.03	1.988	1059.5	0.1		100	1.661	1465.1	0.2
	140.03	3.9344	1089.1	0.1		100	7.244	1507.4	0.2
	140.03	5.8991	1117.9	0.1		150	7.263	1036.6	0.2
	140.03	7.8932	1145.3	0.1		150	3.02	962.1	0.2
	140.03	9.788	1169.5	0.1	Baidakov *et al.*	150	4.001	980.7	0.2
	155.43	2.1451	872.9	0.1		150	2.045	942.1	0.3
	155.43	3.9811	915.1	0.1		160	3.998	861.2	0.3
	155.43	5.9295	954.5	0.1		160	2.043	809	0.3
	155.43	7.8426	990.5	0.1					
	155.43	9.7779	1022.5	0.1					

Table 5: Available values of speed of sound in liquid methane for T between (100 and 160) K and for pressure up to 10 MPa.

only exception is a single point provided by Singer. In this range of temperature, the agreement with the results reported by Van Itterbeek *et al.* is of particular interest, as the previous measurements disagreed, at T = 145 K and at T = 150 K, up to 0.8 % at the lowest pressures [5].

The noticeable improvement in the agreement with Van Itterbeek's measurements is an evidence of how the changes implemented in the measuring cell have led to an improvement in the stability of the measurements at lower temperatures.

In addition to the data available in literature, the experimental results have been also compared with the speed of sound values predicted by two formulation: the fundamental equation of state of methane by Setzmann and Wagner [15] and GERG-2008 [16]. The results of these comparisons are plotted in figure 8 and figure 9, respectively. The Setzmann and Wagner's equation of state has an estimated uncertainty for speed of sound that varies from 0.15 %, for temperatures above 150 K, to 0.3 % at lower temperatures. In the same way, the uncertainty of GERG-2008 formulation ranges from 0.5 %, above 150 K, to 1 % at lower temperatures. Considering the uncertainties of the equations of state and the uncertainty associated with the experimental measurements, it can be seen that all the speeds of sound value obtained in this work are in agreement with predictions of both the formulations.

The larger deviations occur for measurements at 162 K, at lower pressures, where the measurements deviate from the predictions of the mathematical models between (0.3 and 0.4) %. Despite this, even these results are largely within the declared uncertainty.

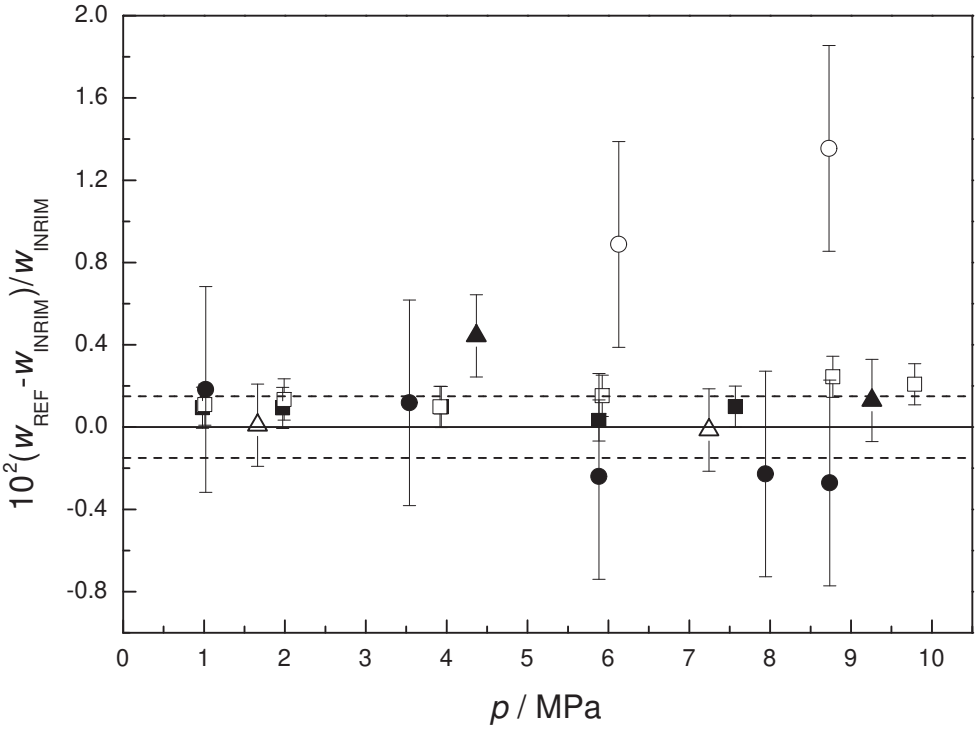

Figure 6: Comparison between experimental speed of sound (with an expanded uncertainty $U(w)$=0.15 %) and available data for temperature below 130 K . (■) Van Itterbeek *et al.*, T = 111 K; (□) Van Itterbeek *et al.*, T = 125 K; (○) Singer, T = 112 K; (●) Singer, T = 125 K; (△) Straty, T = 100 K; (▲) Straty, T = 120 K.

7. Conclusions

The aim of this work was to substantiate, with experimental measurements, the possibility to develop a transfer standard for speed of sound measurement to be used as possible alternative method for the calibration of ultrasonic flowmeters. A transfer standard will allow both to verify, *on-site*, the stability of gauges and it will open to the opportunity to use the speed of sound measured values for a traceable monitoring the quality of the transferred fluid.

The laboratory experimental apparatus used for the speed of sound measurement has, therefore, been characterised in the temperature range between (100 and 162) K and for pressures from (1 to 10) MPa and it has been demonstrated that fully traceable experimental speed of sound are possible at cryogenic conditions also.

These experiments allowed to identify and to resolve the imperfections of the measurement cell as proved by the increased repeatability and the better relative uncertainty, passing from 0.42 % of Cavuoto *et al.* [5] to 0.15 % of this work.

Though further improvements of the performances of the measurement cell will not be achieved in next few years, the actual measurement capabilities already allow to start exploring the new applications derived by availability of a traceable transfer standard for speed of sound measurements.

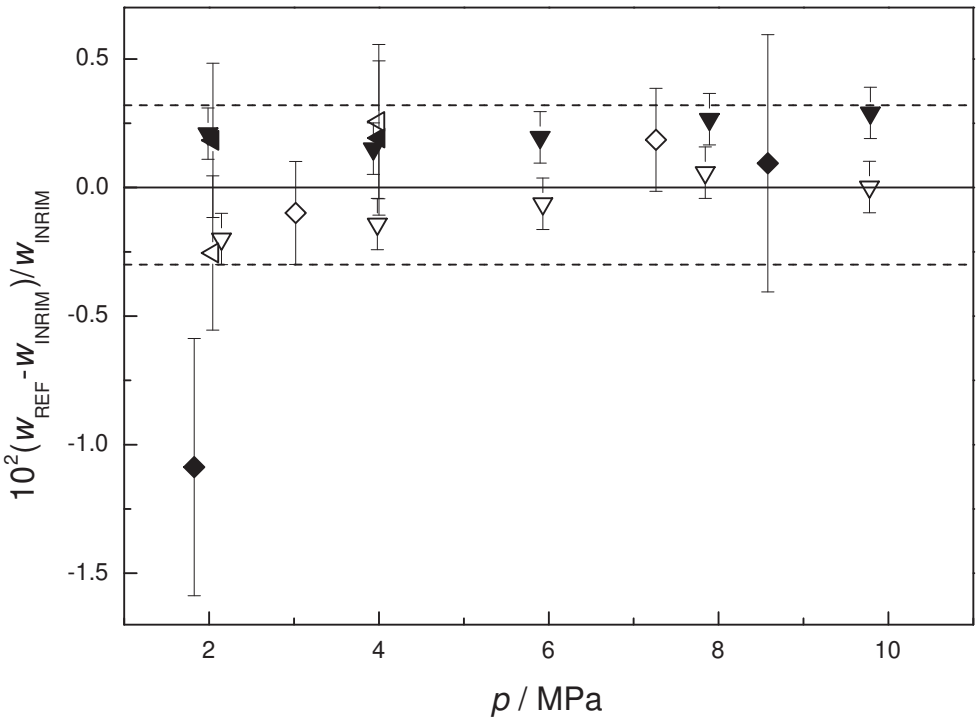

Figure 7: Comparison between experimental speed of sound (with an expanded uncertainty $U(w)$=0.32 %) and available data for temperature above 130 K. (▼) Van Itterbeek *et al.*, T = 140 K; (▽) Van Itterbeek *et al.*, T = 155 K; (●) Singer, T = 145 K; (◇) Straty, T = 150 K; (◄) Baidakov *et al.*, T = 150 K; (◁) Baidakov *et al.*, T = 160 K.

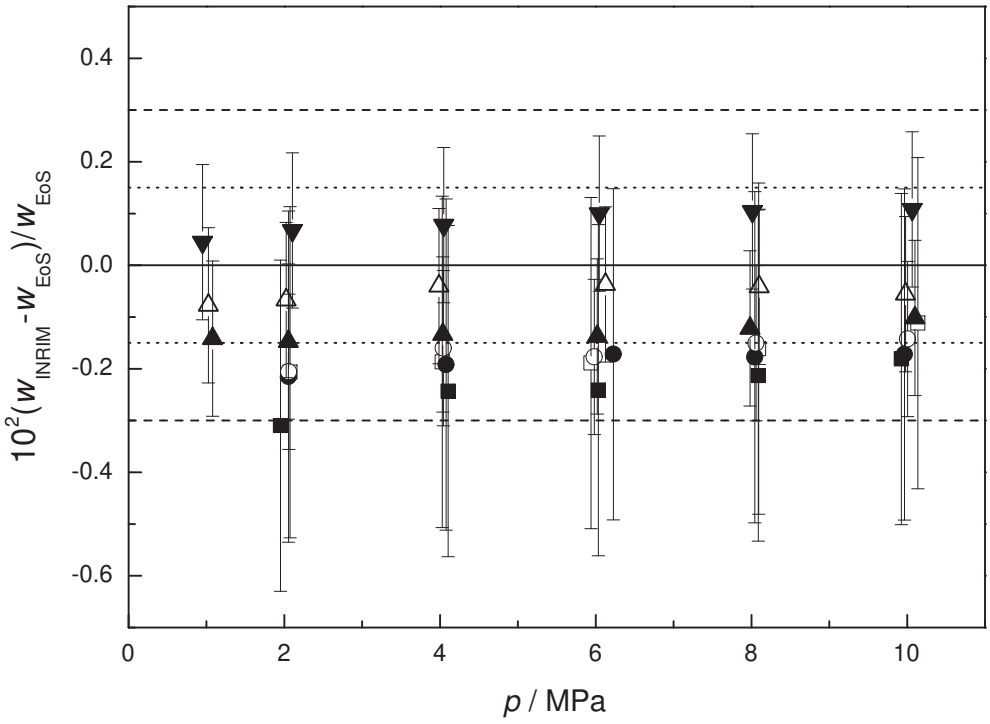

Figure 8: Comparison between experimental speed of sound (with an expanded uncertainty $U(w)$=0.32 % for T > 130 K and $U(w)$=0.15 % for T < 130 K) and predicted values provided by the Setzmann and Wagner equation of state. (▼) T = 100 K; (△) T = 110 K; (▲) T = 120 K; (○) T = 130 K; (●) T = 140 K; (□) T = 150 K; (■) T = 162 K. (. . .) Declared speed of sound uncertainty by Setzmann and Wagner, $u(w)$ = 0.15 % for T > 150 K. (- -) Declared speed of sound uncertainty by Setzmann and Wagner, $u(w)$ = 0.30 % for T < 150 K.

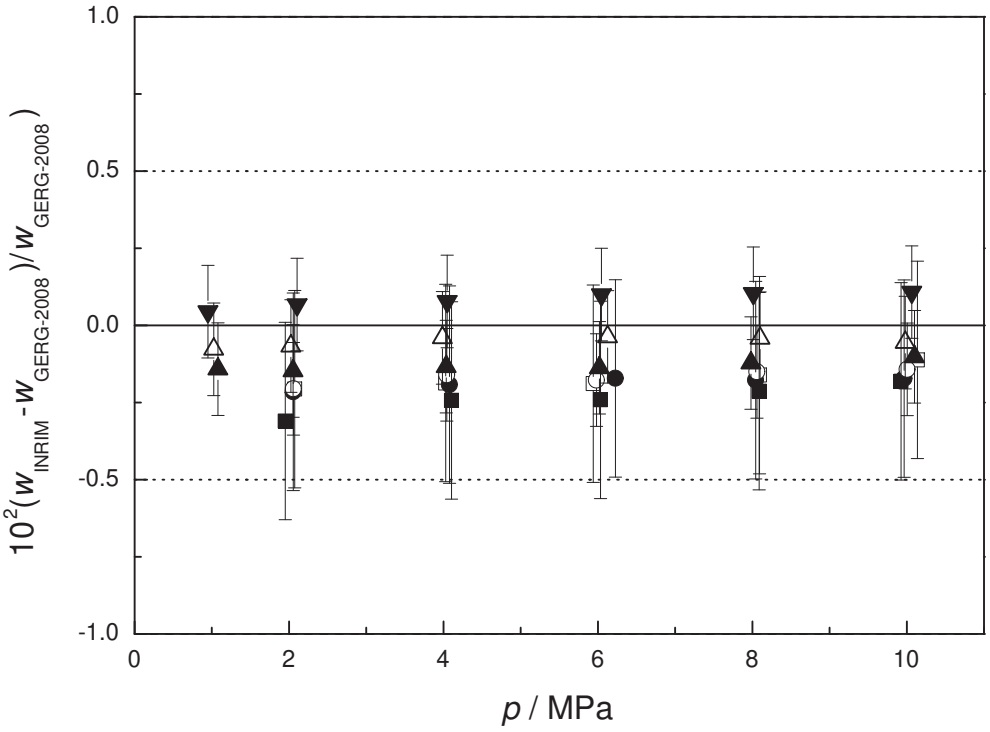

Figure 9: Comparison between experimental speed of sound (with an expanded uncertainty $U(w)$=0.32 % for T > 130 K and $U(w)$=0.15 % for T < 130 K) and predicted values provided by the GERG-2008 model. (▼) T = 100 K; (△) T = 110 K; (▲) T = 120 K; (○) T = 130 K; (●) T = 140 K; (□) T = 150 K; (■) T = 162 K. Declared speed of sound uncertainty by GERG-2008, $u(w)$ = 0.5 % for T > 150 K. (- -) Declared speed of sound uncertainty by GERG-2008, $u(w)$ = 1 % for T < 150 K.

Acknowledgements

This project (16ENG09-LNG3) has received funding from the EMPIR programme co-financed by the Participating States and from the European Union's Horizon 2020 research and innovation programme.

The authors are grateful to all who have contributed to this work, especially to Marco Bertinetti for his valuable help in designing and manufacturing new components of the experimental apparatus. A special thanks also goes to Emanuele Audrito, Elio Keith Bertacco and Stefano Pavarelli for having ensured the regular supply of liquid nitrogen.

References

[1] ISO Standard 12242, "Measurement of fluid low in closed conducts – Ultrasonic transit-time meter for liquid", 2012.

[2] M. Van der Beek, P. Lucas, O. Kerkhof, M. Mirzaei and G. Blom, Results of the evaluation and preliminary validation of a primary LNG mass flow standard, Metrologia **51**(5), 2014.

[3] T. Kegel, The NIST/CEESI Liquid Nitrogen Flow Facility, European Flow Measurement Workshop, Metrology for LNG, April 2017.

[4] G. Benedetto, R. M. Gavioso, P. A. Giuliano Albo, S. Lago, D. Madonna Ripa, R. Spagnolo, Speed of Sound in Pure Water at Temperatures between 274 K and 394 K and at Pressures up to 90 MPa, International Journal of Thermophysics **26**(6), 2005.

[5] G. Cavuoto, S. Lago, P. A. G. Albo, D. Serazio. Speed of sound measurements in liquid methane (CH4) at cryogenic temperatures between (130 and 162) K and at pressures up to 10 MPa. The Journal of Chemical Thermodynamics, 142, 106007 (2020)

[6] H. B. Dixon , C. Campbell and A. Parker, On the velocity of Sound in Gases at High Temperatures, and the Ratio of the Specific Heats, Proc. R. Soc. Lond. 100, 1-26 (1921)

[7] A. Van Itterbeek and L. Verhaegen , Measurments of the Velocity of Sound in Liquid Argon and Liquid Methane, Proc. Phys. Soc. 62, 800 (1949)

[8] W.Van Dael, A. Van Itterbeek, J.Thoen, A.Cops, Sound Velocity Measurements in Liquid Methane, Physica 31, 1643 (1965)

[9] Yu P. Balgoi, A.E. Buko, S.A. Mikhailenko, V.V. Yakuba, Velocity of sound in liquid Kripton, Xenon, and Methane, Russ. J. Chem. 41, 908 (1967)

[10] B. E. Gammon and D. R. Douslin, The velocity of sound and heat capacity in methane from nearcritical to subcritical conditions and equation of state implications, J of Ch. Ph. 64, 203 (1976)

[11] A. Van Itterbeek, J. Thoen, A. Cops and W. Van Dael, Sound Velocity Measurements in Liquid Methane as a Function of Pressure, Physica 35, 162-166 (1967)

[12] J. R. Singer, Excess Ultrasonic Attenuation and Volume Viscosity in Liquid Methane, J. of Ch. Ph. 51, 4729 (1969)

[13] G. C. Straty, Hypersonic velocities in saturated and compressed fluid methane, Cryogenics 15, 729 (1975)

[14] V. G. Baidakov and A. m. Kaverin, Measurement of ultrasonic speed in stable and metastable liquid methane, J. of Ch. Ph. 14, 1003 (1982)

[15] U. Setzmann and W. Wagner, A New Equation of State and Tables of Thermodynamic Properties for Methane Covering the the Range from the Melting Line to 625 K at Pressures up to 1000 MPa, Journal of Physical and Chemical Reference Data 20, 1061 (1991)

[16] O. Kunz and W. Wagner, The GERG-2008 Wide-Range Equation of State for Natural Gases and Other Mixtures: An Expansion of GERG-2004, J. Chem. Eng.,57, 11, 3032-3091 (2012)

[17] J.P.M. Trusler, Physical Acoustics and Metrology of Fluids, Adam Hilger, Bristol, 1991.

[18] R. Wegge, M. Richter, R. Span, Speed of sound measurements in deuterium oxide (D2O) over the temperature range from (278.2 to 353.2) K at pressures up to 20 MPa, Fluid Phase Equilibria **418**, 2016.

[19] A.El Hawary, K.Meier, Measurements of the speed of sound in liquid and supercritical ethane, Fluid Phase Equilibria **418**, 2016.

[20] R. J. Corruccini and J. J. Gniewck, Thermal expansion of technical solids at low temperatures : a compilation from the literature, National Bureau of Standards. Washington, DC, US. Gov. Printing Office 24, (1961).

[21] P. A. Giuliano Albo, S. Lago, R. Romeo, S. Lorefice, High pressure density and speed-of-sound measurements in n-undecane and evidence of the effects of near-field diffraction, Journal of Chemical Thermodynamics **58**, 2013.

[22] H. Preston-Thomas, The International Temperature Scale of 1990 (ITS90), Metrologia 27, 3 (1990).